CHAPTER IV

RESULTS AND DISCUSSIONS

The GaAs-thin-capping and regrowth InAs-QDs at low temperature on the conventional QDs for several cycles are a key process in extending nanopropeller length. Both thin-capping thickness and number of cycles are the combined parameters of thin-capping and regrowth process in growing long chain QDMs. In order to clearly analyze the AFM images of nanostructure, nanopropeller structures ,which is template for growing QDMs, is systematically studied. Proper InAs regrowth thickness in the last cycle, which is the final process of QDMs growth, is identified. PL measurement is conducted to determine the characteristics of QDMs structure as well as the optical anisotropic property of QDMs.

4.1 Nanopropeller Structure Investigation

After oxide desorption under As_4 overpressure of 8×10^{-6} Torr, a 300 nm of GaAs buffer layer was grown on GaAs(100) substrates with growth rate of 0.6 ML/s at 580°C. Afterward, the substrates were cooled down to 500°C. This temperature, which was used as a reference temperature, was checked by RHEED-pattern transition from (2x4) to (2x2) reconstruction. 1.8 ML of InAs was deposited to form QDs using low growth rate of 0.01 ML/s. The growth interruption time of 30s was applied to obtain uniform QDs (in Fig. 4.4 a)) before the substrate temperature was reduced to 470°C. The QDs were thin-capped by GaAs with different thicknesses and the growth interruption of 25 s was applied at retaining temperature of 470°C. During the interruption time, In atoms of dots segregate to regions outside of the QDs. Nanohole structures are created after the growth interruption. After that, InAs QDs were regrown on nanohole structures with different requirements of InAs thicknesses. The thicker thin-capping thickness was deposited, the more InAs amount was required to form QDs. The thickness was estimated by observing RHEED transition into clear spotty pattern. As the results, the InAs thicknesses necessary for QDs formations on samples thin-capped with 6, 9, 12 and 15 ML of GaAs are 0.6, 0.75,

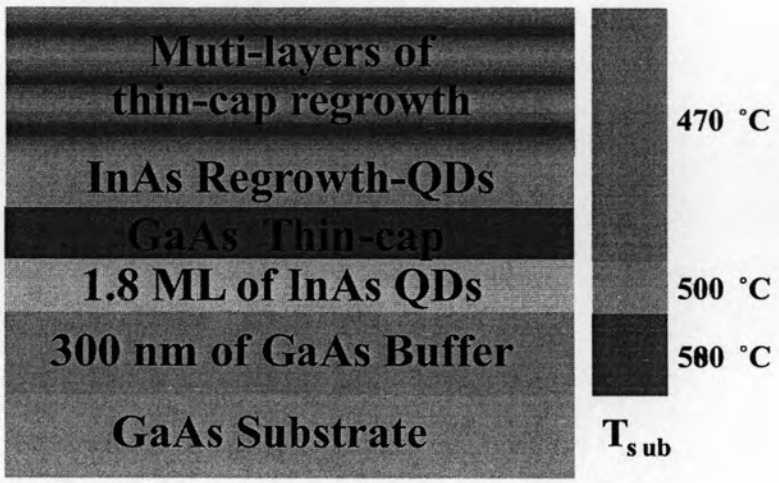

Figure 4.1: Block diagram and growth temperature of samples for nanopropeller investigation

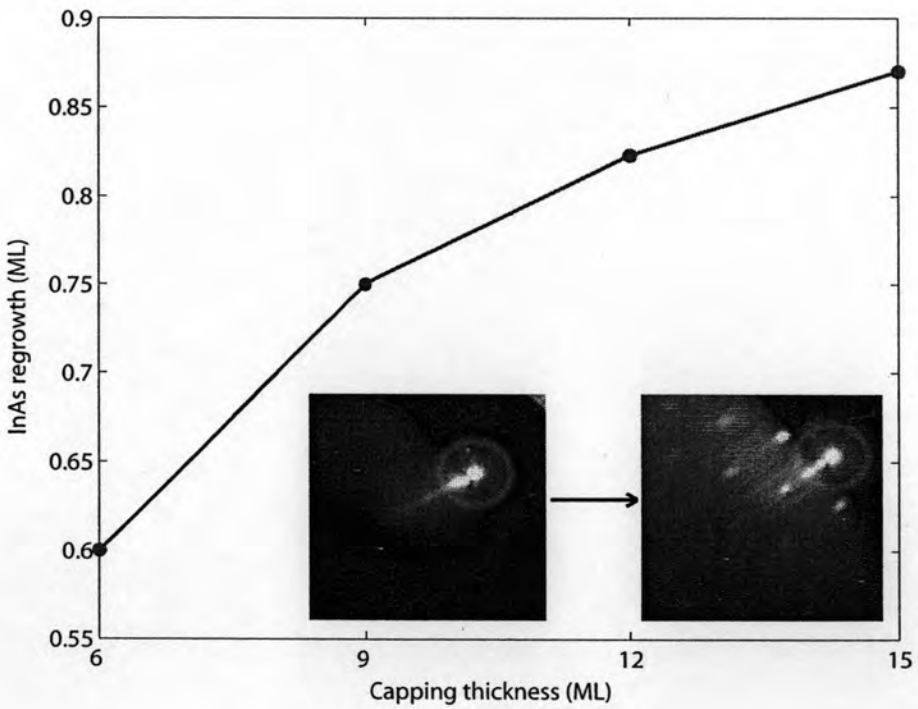

Figure 4.2: The InAs regrowth thickness sufficient to form QDs on GaAs thin-capping layer whereby the thickness was estimated by observing RHEED transition into clear spotty pattern.

0.82 and 0.875 ML, respectively, as shown Fig. 4.2. These different requirements of InAs regrowth thickness are arised from different InGaAs composition of nanohole structures. Thicker thin-capping layer leads to higher InGaAs composition of nanohole structures and thus require thicker InAs regrowth thickness. After QD-regrowth and annealing for 25 s, the QDs locating at the center of nanopropellers are nucleated above the collapsed QDs in GaAs thin-capping layer due to the seeding effect of strain. It is also found that both of nanopropeller's blades stretch along $[1\bar{1}0]$ crystallographic direction due to strain anisotropy. Thin-capping-and-regrowth processes were done for 1, 3, 5, 7 cycles whereby thin-capping thickness of each cycles is the same as the first cycle. The nanopropeller length measured by AFM is summarized in Table.4.1 and Fig. 4.3. Nanopropeller QDs from 9ML-thin-capping for 1,3,5 and 7 cycles are shown in Fig.4.4 b), c), d) and e) respectively.

Table 4.1: The statistical summary of nanopropeller length

Capping Thickness (ML)	The number of cycles	Average Length (nm)	S.D.
6	1	310.52	21.9
9	1	335.55	22.24
9	3	526.51	93.91
9	5	725.40	98.86
9	7	1005.50	185.60
12	3	502.07	53.05
12	5	695.65	82.72
12	7	944.36	123.56
15	1	227.62	15.44
15	3	487.42	82.96
15	5	554.05	132.34
15	7	847.17	197.36

Corresponding to all thin-capping thicknesses, the nanopropeller length is increased when more capping-and-regrowth process is repeated. Considerably, the length of nanopropellers with thin-capping thickness of 9 ML is consistently longer than the length of nanopropeller with thin-capping thickness of 12 and 15 ML. However, the length fluctuation of nanopropeller from several cycles of thin-capping-and-regrowth is lowest at thin-capping thickness of 12 ML and is highest at thin-capping thickness of 15 ML.

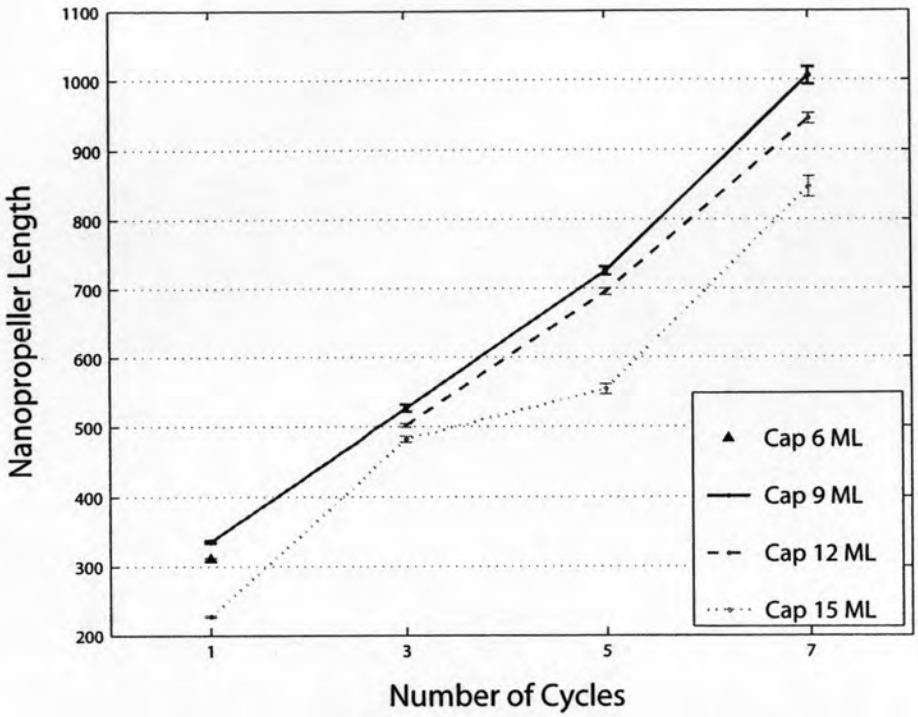

Figure 4.3: Summary of nanopropeller length as function of cycles of thin-capping-and-regrowth for thin-capping thickness of 6, 9, 12 and 15 ML

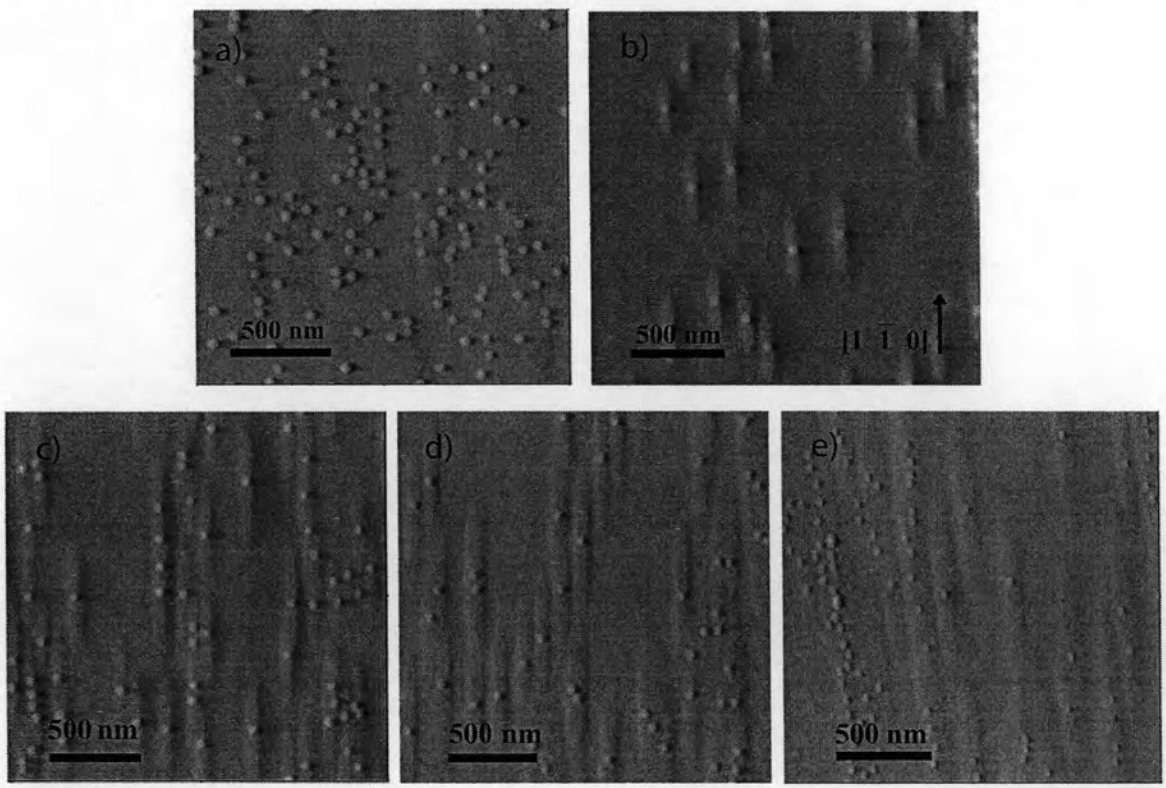

Figure 4.4: AFM images of as-grown QDs a) and nanopropeller from 1, 3, 5 and 7 cycles of thin-capping-and-regrowth b), c), d) and e), respectively

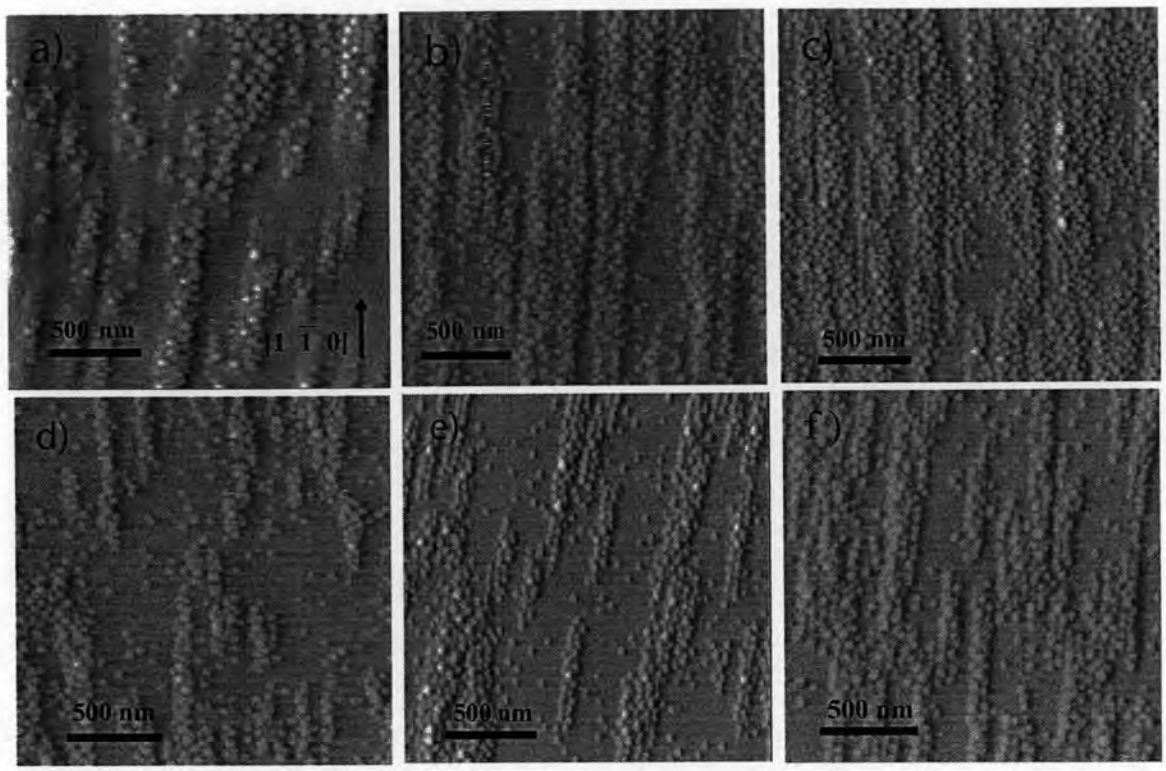

Figure 4.5: AFM images of QDMs from 5 cycles of 9ML-thin-capping-and-regrowth with final-regrowth thickness of 1.3, 1.6 and 1.8 ML (in a), b) and c),respectively), QDMs from 1 and 3 cycles (in d) and e)) of 9ML-thin-capping-and-regrowth with final-regrowth thickness of 1.2 ML and 1.6 ML,respectively. And QDMs from 5 cycles of 12ML-thin-capping-and-regrowth and final-regrowth thickness of 1.6 ML (in f))

4.2 Quantum Dot Molecules

QDMs can be attained by depositing further InAs in the last cycles. The additional QDs, called satellite QDs, are likely to locate on the nanopropeller's blades as the strained templates. As the results, amount of satellite QDs increases with the regrowth thickness. The QDMs from 1 cycle with thin-capping thickness of 9 ML and regrowth thickness of 1.2 ML contain about 9 satellite QDs in average or 10 QDs including centre dot in a group (Fig. 4.5 d)). And the QDMs from 5 cycle with thin-capping thickness of 9ML contain 11 and 25 satellite QDs for 1.3 and 1.5 ML of final-cycle regrowth thicknesses (Fig. a) and b), respectively). For final-cycle regrowth thickness of 1.8 ML, they are uncountable due to too high density of QDs (Fig. 4.5 c)). It is almost impossible to find QDMs which are originated from isolated nanopropeller. The number of QDs are corresponding to the nanopropeller length. Longer nanopropeller template can be attained the longer

chain of QDMs by sufficient final regrowth thickness. Although the number of QDs on the template increases with thicker final regrowth, number of QDs outer the templates also increased. It means that final-regrowth thickness should be properly used. In case of thin-capping thickness of 9 ML, final regrowth with thickness increasing from 0.75 ML to 1.6 ML yields numbers of QDs from 1 to 25 QDs. However, when the thickness is increased up to 1.8 ML, QDs become high density due to increasing of QDs outside nanopropeller. If we consider in term of density of QDs, QDMs chains increase from densities of as-grown QDs ($3.21 \times 10^9 cm^{-2}$) and nanopropeller QDs ($1.8 \times 10^9 cm^{-2}$) to $1.07 \times 10^{10} cm^{-2}$, $2.7 \times 10^{10} cm^{-2}$ and $3.38 \times 10^{10} cm^{-2}$ for final-cycle regrowth thicknesses of 1.3, 1.6 and 1.8 ML, respectively (Fig. 4.5 a), b) and c)). It is clear that thicker InAs thickness which is deposited in final-regrowth results in higher density. And longer nanopropeller templates are capable to thicker InAs deposition in final-regrowth with less QDs outside templates.

Table 4.2: The statistical summary of quantum dot molecules

Capping Thickness (ML)	The number of cycles	Final-cycle Regrowth Thickness (ML)	Number of QD per Group	QD Density
9	1	1.2	9.6	$1.94 \times 10^{10} cm^{-2}$
9	3	1.6	18.57	$2.22 \times 10^{10} cm^{-2}$
9	5	1.3	10.18	$1.07 \times 10^{10} cm^{-2}$
9	5	1.6	24.75	$2.70 \times 10^{10} cm^{-2}$
9	5	1.8	-	$3.38 \times 10^{10} cm^{-2}$
12	5	1.6	22.16	$2.24 \times 10^{10} cm^{-2}$

4.3 Photoluminescence of Quantum Dot Molecules

QDMs samples for PL measurement were capped with 10 nm of GaAs at final QDs regrowth temperaure of 470 °C. And the substrate temperature was ramped up to 500 °C while the growth of GaAs was suspended. Further 90 nm of GaAs was grown when substrate temperature was stable. While, as-grown QDs sample were capped with 100 nm of GaAs at QDs growth temperaure of 500 °C. All samples drown in cryostat filled with liquid nitrogen to keep the samples temperature at 77 K during measurements. And the samples are excited by Ar^+ laser at wavelength of 488 nm (2.541 eV).

The QDMs from 1 cycle of 9ML-thin-capping-and-regrowth (Fig. 4.5 d)) and from 5 cycles of 9ML-thin-capping-and-regrowth (Fig. 4.5 b) and c)) were studied by photoluminescence. Peaks of PL spectra are at 1.081, 1.130 and 1.167 eV for as-grown QDs (with excitation power = 200 mW), QDMs from 1 and 5 cycles of 9ML-thin-capping-and-regrowth (with excitation power = 80 mW), respectively. The emission energies of PL peaks relate to size of QDs of each samples. The height of as-grown QDs measured by AFM line scan is 6.25 nm. The QDMs from 1 (5) cycles consist of two sizes. They are 5.17 (5.97) nm for the height of centre QDs and 2.90 (3.60) nm for the height of satellite QDs. The peak positions of QDMs locate at energies higher than of the position of as-grown QDs due to smaller size of QDs and also due to capping at lower temperature in the first-stage. The dot heights of QDMs from 5 cycles of thin-capping-and-regrowth is greater than QDMs from 1 cycles of thin-capping-and-regrowth because of thicker regrowth thickness. But the emission energy of QDMs from 5 cycles of thin-capping-and-regrowth is higher than that from 1 cycle because number of satellite QDs ratio to centre QDs of a QDM from 5 cycles is greater. The number of satellite QDs ratio to centre QDs is 9.78 for 1 cycle and becomes 14.0 for 5 cycles. For QDMs from 9ML-thin-capping-and-regrowth for 5 cycle and 1.8ML-final-regrowth (Fig. 4.5 c)), PL spectra (Fig. 4.7) are almost same as QDMs from 5 cycle of thin-capping-and-regrowth with 9 and 12 ML of thin-capping thickness and 1.6ML of final-regrowth. Their peak positions are around 1.65-1.70 eV with FWHM around 48.5-51 meV.

Emission spectrum of as-grown QDs is the narrowest which indicates good uniformity of as-grown QDs. Full width at half maximum (FWHM) is used to express degree of broadening. FWHM of as-grown QDs, QDMs from 1 cycle and 5 cycles of 9ML-thin-capping-and-regrowth are 33, 113.5 and 51 meV. Highly broadening of QDMs from 1 cycle of thin-capping-and-regrowth is resulted from two different sizes of QDs and emission of first excited state also incorporated. Peak of first excited energy was found at 1.19 eV at power excitation of 80 mW. It was revealed by varying excitation power (Fig. 4.8). When excitation power was increased, PL intensity of first excited state increased relatively to intensity of ground state. It was also found in as-grown QDs at 1.14 eV at excitation power of 200 mW but this peak is small comparing to the ground state (Fig. 4.9 a)). QDMs from 12ML-thin-capping-and-regrowth for 5 cycles (Fig. 4.5 d)), which

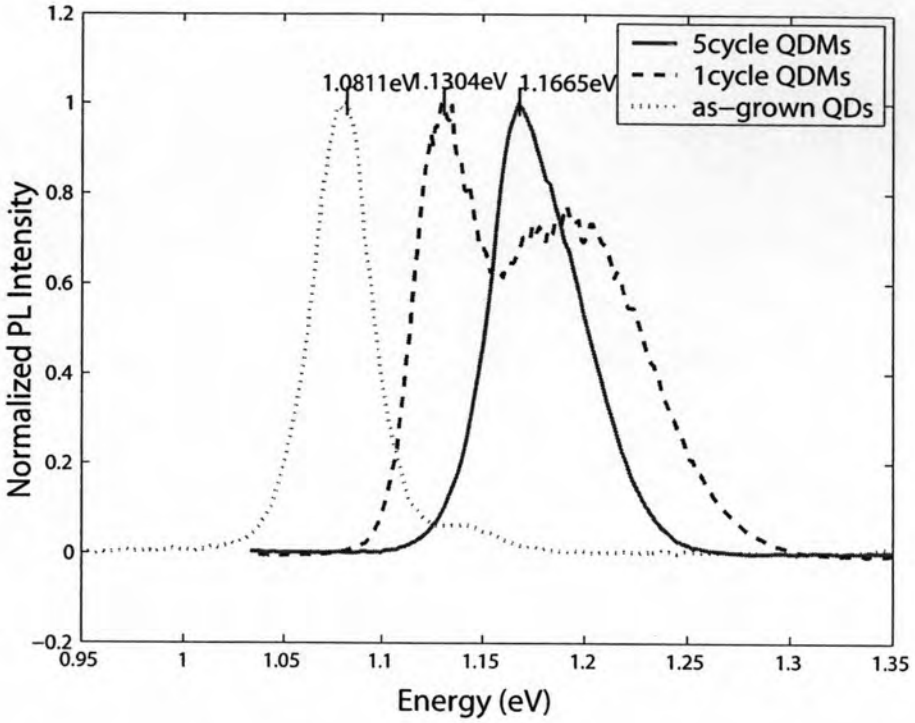

Figure 4.6: Normalized PL Spectrum of as-grown QDs (Fig. 4.4 a)) and QDMs from 1 and 5 cycles of thin-capping-and-regrowth (Fig. 4.5 d) and b)) at 77 K

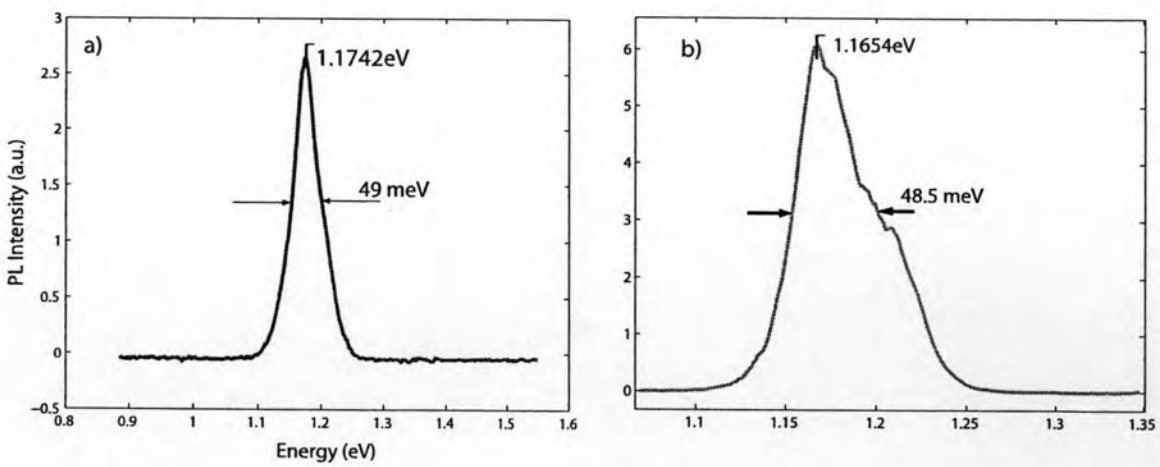

Figure 4.7: a) PL spectrum of QDMs from 12ML-thin-capping-and-regrowth for 5 cycles and 1.6ML-final-regrowth (Fig.4.5 f)) and b) PL spectrum of QDMs from 9ML-thin-capping-and-regrowth for 5 cycles and 1.8ML-final-regrowth (Fig. 4.5 c))

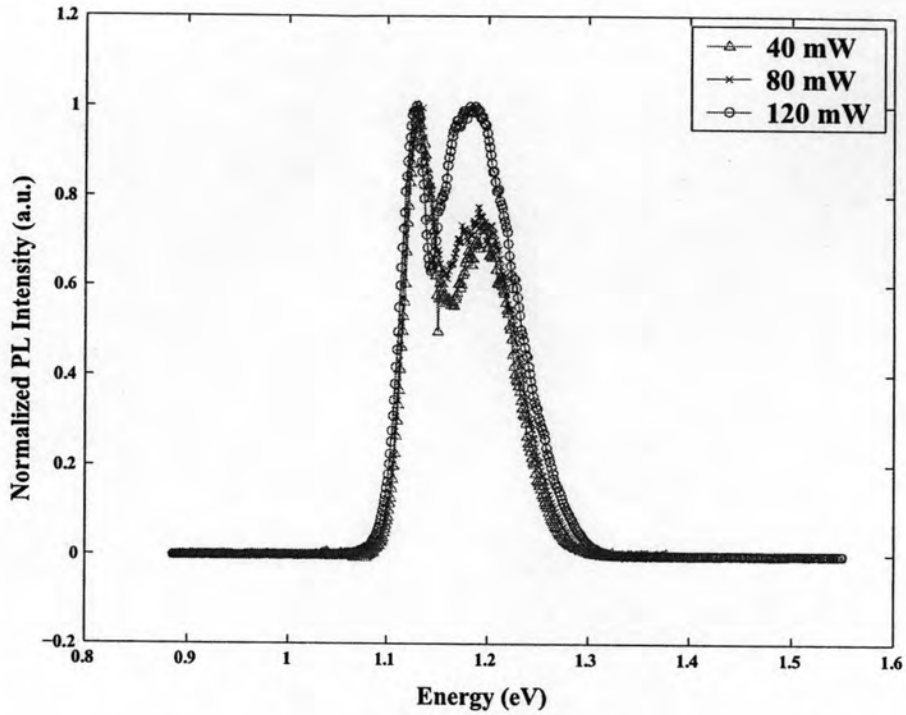

Figure 4.8: Normalized PL Spectrum of QDMs with thin-capping of 9 ML for 1cycles with different excitation power at 77 K

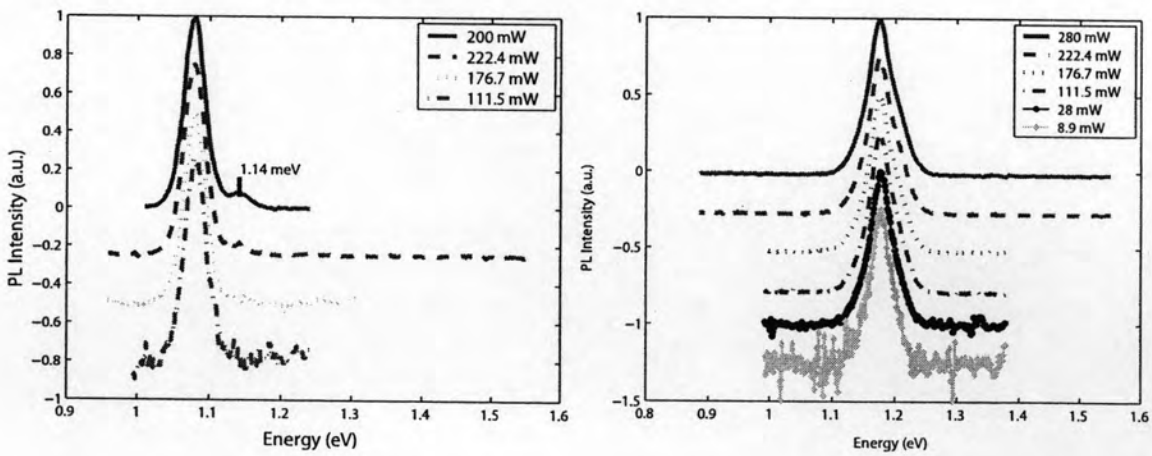

Figure 4.9: Normalized PL Spectrum of as-grown QDs a) and QDMs from 12 ML-thin-capping-and-regrowth for 5 cycles b) with different excitation power at 77 K

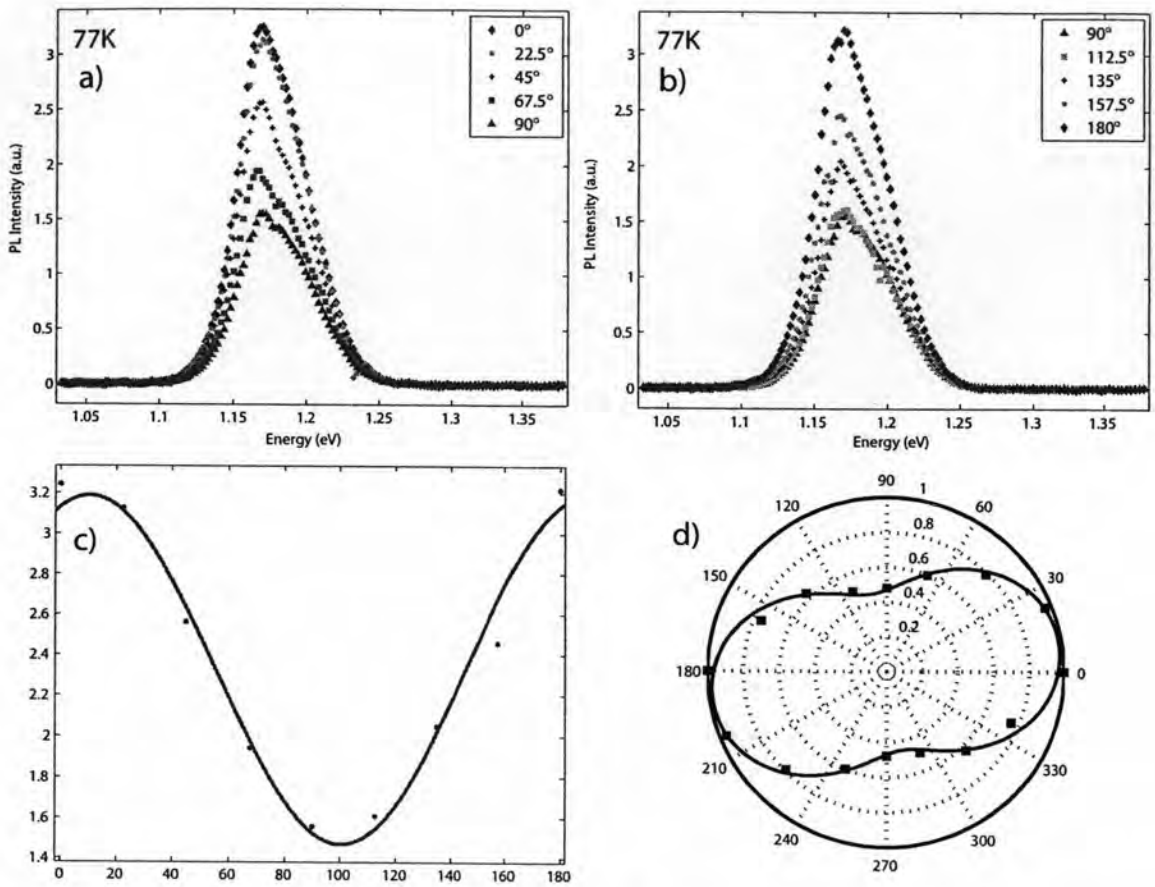

Figure 4.10: PL spectrum of QDMs from 9ML-thin-capping and regrowth for 5 cycles and 1.6MLfinal-regrowth which polarized in angle of 0° to 90° a) and in angle of 90° to 180° b). c) and d) show peaks intensity as a function of polarized angle in x-y coordinate and polar coordinate, respectively

have the peak position at 1.174, does not give the PL peak of first excited state as shown in Fig.4.9 b). Their broadening of PL spectrum are resulted mainly from non-uniform QDs size.

4.4 Polarization Dependence of Photoluminescence

The polarization of laser beam was adjusted by retarding a halfwave plate. A polarizer was used to filter light emerging from the samples before the light entered into monochromator. The polarization of laser was adjusted to obtain the highest excitation of electron in QDMs by observing PL intensity at the peaks. After that, the polarizer was retarded to determine the highest intensity and we set that direction to be angle of

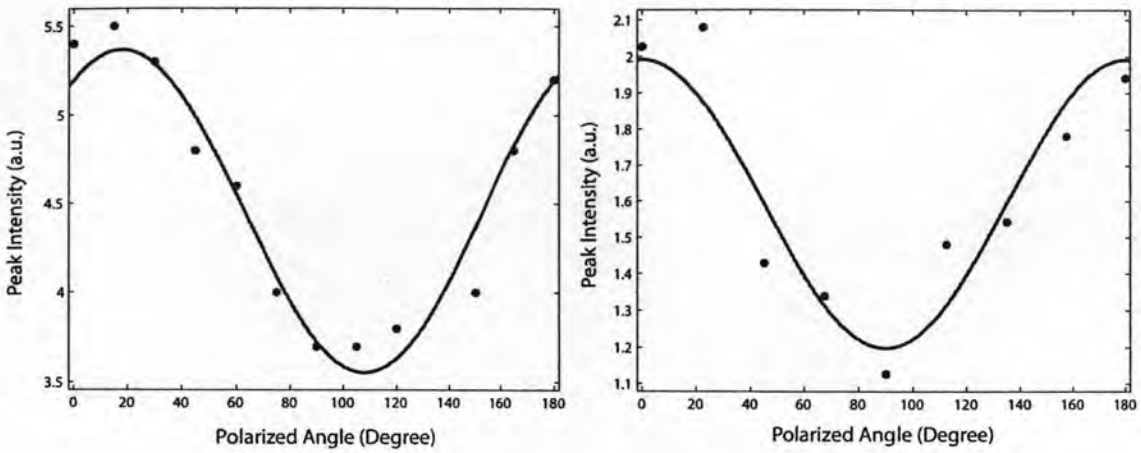

Figure 4.11: Polarization dependence of peak intensity of QDMs from 9ML-thin-capping and regrowth for 5 cycles and 1.8MLfinal-regrowth a) 12ML-thin-capping and regrowth for 5 cycles and 1.6MLfinal-regrowth b)

zero. The polarizer was retarded to several angles against the zero angle and PL spectra were scanned. Polarization dependences of PL spectra were observed in QDMs from 5 cycles of thin-capping-and-regrowth both with 9 and 12 ML of thin-capping thicknesses but not found in as-grown QDs and QDMs from 1 cycles of thin-capping-and-regrowth. Polarization dependence of PL spectrum of QDMs from 5 cycles of 9ML-thin-capping-and-regrowth is shown in Fig. 4.10. Intensity of PL spectrum decreases when the polarizer is varied from 0° to 90° and increased when the polarizer are retarded from 90° to 180°. Peak intensities at different angles of polarizer are plotted to determine the degree of polarization (P) which is defined as:

$$P = \frac{I_{max} - I_{min}}{I_{max} + I_{min}}, \tag{4.1}$$

where I_{max} and I_{min} are the maximum and minimum PL intensity. The degree of optical polarization anisotropy of QDMs are summerized in Table. 4.3

Table 4.3: The degree of optical polarization anisotropy (DOPA) of quantum dot molecules

Capping Thickness (ML)	Cycles	Final-cycle Regrowth Thickness (ML)	DOPA (P)	A	B	B/A	$\delta(^\circ)$
9	5	1.6	35.15%	3.187	1.470	0.46	10.44
9	5	1.8	21.35%	5.368	3.555	0.662	17.95
12	5	1.6	29.72%	1.992	1.198	0.601	-0.085

The optical anisotropy of QDM chains is resulted from the difference in the square of the magnitude of the wave vectors between $[1\bar{1}0]$ and $[110]$ directions ($k^2_{[1\bar{1}0]}, k^2_{[110]}$). It is arised from the difference in amount of coupled QDs in each direction. The measurement results of the peaks of PL spectrum can be comparatively explained. QDMs from 5 cycles of 9ML-thin-capping-and-regrowth and 1.6ML- final regrowth (Fig. 4.5 b)) have stronger polarization dependence photoluminescence than QDMs from 5 cycles of 12ML-thin-capping-and-regrowth (Fig. 4.5 b)). That is in an agreement with the length of nanopropeller templates that they are longer. It implies that the number of coupled QDs aligning along $[1\bar{1}0]$ direction is greater. In contrast, QDMs from 5 cycles of 9ML-thin-capping-and-regrowth and 1.8ML- final regrowth have weaker optical anisotropy than the others, because it have too high density of QDs which lead to greater amount of coupling in $[110]$ direction. So the anisotropic alignment is reduced. The result was confirmed by PL measurement of long chain QDMs from lower density of as-growm QDs which thier AFM image is shown in Fig 4.12 whereby thier QDs density is $1.56 \times 10^{10}\mathrm{cm}^{-2}$. The degree of optical polarization is high up to 63% as shown in Fig 4.13.

The results of peak intensity of PL spectrum exhibit existence of two orthogonal components of PL peak intensity. The peak intensity of PL spectrum was thus fitted by

$$I = A\cos^2(\theta - \delta) + B\sin^2(\theta - \delta), \tag{4.2}$$

or

$$\mathrm{normalized}I = \cos^2(\theta - \delta) + \frac{B}{A}\sin^2(\theta - \delta), \tag{4.3}$$

where A and B correspond to the peak intensities of PL spectrum in each of their component, θ is polarization angle and δ corresponds to the deviation angle due to zero-angle setting error. All fitting parameters (by using curve fitting tool, MATLAB 6.5) are shown in Table. 4.3.

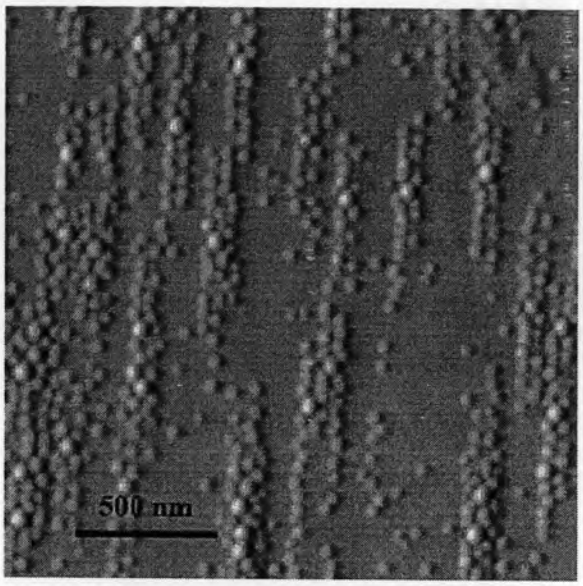

Figure 4.12: AFM images of QDMs from 12ML-thin-capping and regrowth for 5 cycles and 1.6 ML of final-regrowth thickness

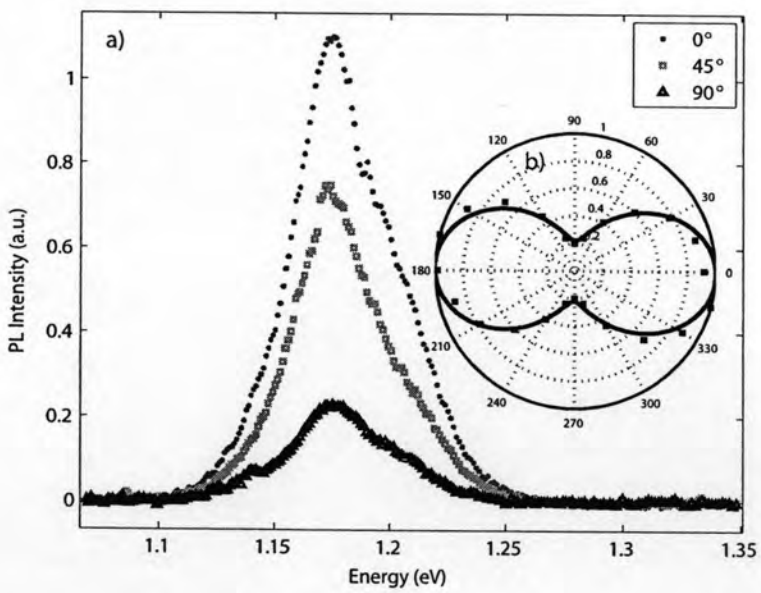

Figure 4.13: PL spectrum of QDMs from 12ML-thin-capping and regrowth for 5 cycles and 1.6ML of final-regrowth thickness which polarized in angle of 0° to 90° a) and b) show peaks intensity as a function of polarized angle, respectively